POLITECNICO DI TORINO
Repository ISTITUZIONALE

An improved calibration technique for on-wafer large signal characterization

Terms of use:

Publisher copyright

(Article begins on next page)

27 November 2024

An Improved Calibration Technique for On-Wafer Large-Signal Transistor Characterization

Andrea Ferrero and Umberto Pisani

Abstract—The on-wafer measurement of complex quantities and absolute power levels of active devices are truly significant for nonlinear device characterization and modeling. In this paper, an original procedure, which allows one to perform both the vector and the power calibrations at the RF wafer probe tips used for on-wafer measurement of two port devices, is presented.

The measurement system is based on an automatic vector network analyzer with coaxial directional couplers and RF coplanar wafer probes. A new error model of the dual directional coupler, which samples the power waves traveling at device output, allows one to take advantage of the coaxial section at the output of the measuring system for calibrating the power level up to the on-wafer probe tips.

I. INTRODUCTION

A COMPLETE active power device characterization under large signal behavior, carried out directly on wafer, can be accomplished by means of vector "load-pull" techniques [1], [2].

All cited methods require the acquisition of several vector quantities such as device input impedance, load impedance, transfer function, and so on directly at the device pads. In addition to these ratio parameters, an absolute power measurement at the device output port is also required.

The measurement test set, described in the block diagram of Fig. 1, was suggested for coaxial systems by Hetch [3], and a vector network analyzer (NWA) is used to measure both the large signal vector quantities and the power levels. To extend the technique to on-wafer measurements, either an on-wafer power sensor needs to be used[1] or a deembedding procedure has to be carried out to remove the effect of the wafer probes.

In this paper, an overall procedure is presented, which allows one to perform both the vector and the power calibrations at the probe tips without either on-wafer power sensors on probe-deembedding procedures. This result was accomplished by introducing a new error model of the output dual directional coupler which, with respect to [3], extends the use of the coaxial port 5 to power calibration.

[1]On-wafer power sensors are under development [4], but to the authors' knowledge, they are not commercially available yet.

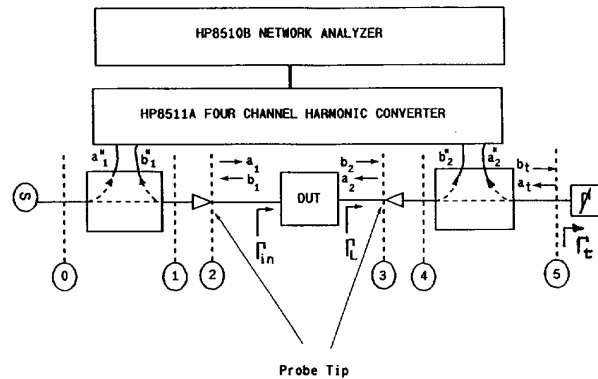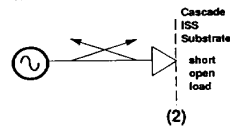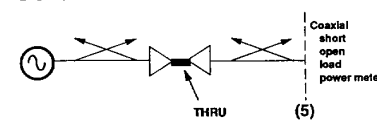Fig. 1. Test set block scheme and reference planes definition.

Fig. 2. Standard connection procedure.

According to the suggested error model, a coaxial power meter connected to port 5 during the calibration provides an absolute power reference value for the whole system up to the on-wafer probe tips.

The suggested technique reduces the number of standard connections with respect to previous ones since it requires three on-wafer standard loads at the input probe tip, and through line between the probe tips, three coaxial standard loads at the output coaxial port (port 5 of Fig. 1), and a power measurement at the same port. Fig. 2 summarizes the standard connections required by this procedure.

The basic theory for calibrating the input and output reflection coefficients along with the new error model will be presented first. Next, the on wafer power calibration will be considered, and finally, the mathematical expressions for vectorial correction of the DUT gain will be derived.

The theory has been applied with good results, to the particular test set of Fig. 1, and more recently to a milli-meter-wave test set a version of which was used success-fully to characterize a MMIC TWA and MODFET's [7].

II. INPUT AND OUTPUT REFLECTION COEFFICIENT CALIBRATION

A. Input Port

To calibrate the reflection coefficient at the input port of the DUT (i.e., at port 2, Fig. 1), the well-known one-port error box model, whose flow graph is shown in Fig. 3, is used. The input error coefficients are derived by con-necting three on-wafer standard loads, for example, an open, a short, and a matched load, at the input probe tip [5]. The linear system obtained from three raw reflection measurements allows one to compute the usual one-port error coefficients: Ed_1, Es_1, $Er_1 = I_{10}I_{01}$.

The measured raw input reflection coefficient

$$\Gamma_{in}^M = \frac{b_1^M}{a_1^M} \qquad (1)$$

can be processed to give a corrected Γ_{in} value by means of the well-known equation

$$\Gamma_{in} = \frac{\Gamma_{in}^M - Ed_1}{Er_1 + Es_1(\Gamma_{in}^M - Ed_1)}. \qquad (2)$$

B. Output Port

The output port error box model was modified with re-spect to [3] to provide information on the absolute power levels at the probe tips from a coaxial measurement at port 5 (Fig. 1). Our model, which is fully derived in Appendix A, leads to the two flow graphs of Fig. 4. The graph of Fig. 4(a) links the NWA readings with the traveling waves at port 5, while the graph of Fig. 4(b) gives the relation-ships between the same voltage waves and those at port 3. Note the reciprocity of the network represented by the graph of Fig. 4(b).

The parameters E_{00}, E_{11}, and E_{10}^2 are evaluated by con-necting a known two-port standard between ports 2 and 3 and by using the input reflectometer, previously cali-brated, to measure the leftover part of the test set.

When a through is inserted[2] ports 2 and 3 correspond, and if we connect three standard coaxial loads at port 5, their reflection coefficients shifted back at the probe tip section can be accurately measured with the input reflec-tometer. The unknown coefficients E_{00}, E_{11}, and E_{10}^2 are found by solving the linear system formed from three equations:

$$\Gamma_{ini} = \Gamma_{Li} = E_{00} + \frac{E_{10}^2 \Gamma_{ti}}{1 - E_{11}\Gamma_{ti}} \qquad (3)$$

[2]To simplify the mathematics, a through connection is first considered as a standard, while formulas for the general case of an arbitrary two-port used as a through are derived in Appendix B.
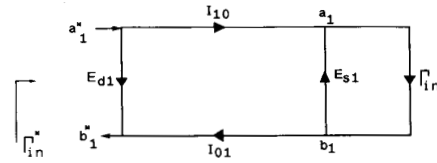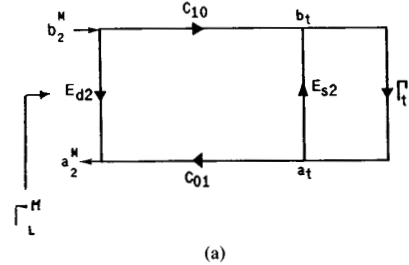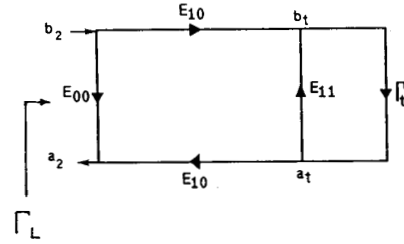

Fig. 3. Input port flow graph.

(a)

(b)

Fig. 4. Output directional coupler flow graph.

where Γ_{ti} ($i = 1, 2, 3$) are the three coaxial standard loads at port 5. These three different standards are also used to compute the error parameters of the flow graph of Fig. 4(a) (Ed_2, Es_2, $Er_2 = C_{10}C_{01}$) which links Γ_t to the mea-sured raw output reflection coefficient:

$$\Gamma_L^M = \frac{a_2^M}{b_2^M}. \qquad (4)$$

Again, the error parameters are obtained by solving a lin-ear system from three equations:

$$\Gamma_{Li}^M = Ed_2 + \frac{Er_2\Gamma_{ti}}{1 - Es_2\Gamma_{ti}}. \qquad (5)$$

When a general load Γ_t is connected to port 5, the re-flection coefficient Γ_L, presented at the output probe tip, is obtained from the measured Γ_L^M by following these steps.

1) Γ_t is computed from the measured Γ_L^M as

$$\Gamma_t = \frac{\Gamma_L^M - Ed_2}{Er_2 + Es_2(\Gamma_L^M - Ed_2)}. \qquad (6)$$

2) Γ_L is obtained from Γ_t from the equation

$$\Gamma_L = E_{00} + \frac{E_{10}^2\Gamma_t}{1 - E_{11}\Gamma_t}. \qquad (7)$$

(Equations (6) and (7) could be combined and Γ_L obtained directly from Γ_L^M, but the relationship (6) is pointed out as Γ_t will occur in further mathematical developments.)

III. CALIBRATION OF THE POWER LEVELS AT PROBE TIPS

A. Power at the Output Probe Tip

From the output flow graphs of Fig. 4, the output power P_L is easily linked to the NWA reading $|b_2^M|^2$ as

$$P_L = |b_2^M|^2 \left|\frac{C_{10}}{E_{10}}\right|^2 \left|\frac{1 - E_{11}\Gamma_t}{1 - Es_2\Gamma_t}\right|^2 (1 - |\Gamma_L|^2). \quad (8)$$

Equation (8) still includes the unknown error coefficient $|C_{10}/E_{10}|^2$.

The parameter $|E_{10}|^2$ is already known from the output port calibration described above, while $|C_{10}|^2$ can be provided by (9) from a power measurement (with a coaxial power meter) at port 5 and from the raw measured value $|b_2^M|^2$:

$$|C_{10}|^2 = \frac{P_{mr}|(1 - Es_2\Gamma_{pm})|^2}{|b_2^M|^2(1 - |\Gamma_{pm}|^2)} \quad (9)$$

where P_{mr} is the power meter reading and Γ_{pm} is the power sensor reflection coefficient at port 5.

B. Power at Input Probe Tip

If a through is inserted between the probe tips (i.e., $a_1 = b_2$), the analysis of the three flow graphs gives

$$b_t = a_1^M \frac{I_{10}E_{10}}{(1 - Es_1\Gamma_{in})(1 - E_{11}\Gamma_t)} \quad (10)$$

so when the power meter is connected at port 5, $|I_{10}|^2$ can be evaluated as

$$|I_{10}|^2 = \frac{P_{mr}|(1 - Es_1\Gamma_{in})|^2|(1 - E_{11}\Gamma_{pm})|^2}{|E_{10}|^2(1 - |\Gamma_{pm}|^2)|a_1^M|^2}. \quad (11)$$

Finally the corrected value of P_{in} can be computed by

$$P_{in} = |a_1^M|^2 \frac{|I_{10}|^2}{|1 - Es_1\Gamma_{in}|^2} (1 - |\Gamma_{in}|^2). \quad (12)$$

IV. VECTOR GAIN CALIBRATION

The NWA is also used to obtain a calibrated value of the vector quantity b_2/a_1. The flow graph analysis gives

$$\frac{b_2}{a_1} \left(\frac{C_{10}}{E_{10}I_{10}}\right) \frac{(1 - Es_1\Gamma_{in})(1 - E_{11}\Gamma_t)}{1 - Es_2\Gamma_t} \left(\frac{b_2^M}{a_1^M}\right). \quad (13)$$

The complex error coefficient

$$E_G = \frac{C_{10}}{E_{10}I_{10}} \quad (14)$$

has to be evaluated in order to calibrate b_2/a_1.

When the through is inserted during the calibration procedure, E_G can be easily obtained from (13) and from the raw (b_2^M/a_1^M) measured data, remarking that $b_2 = a_1$.

TABLE I
COMPARISON BETWEEN POWER METER ($P1$) AND NWA ($P2$)
MEASUREMENTS AT PORT 1

$F = 10$ GHz		$F = 14$ GHz		$F = 18$ GHz	
$P1$ (dBm)	$P2$ (dBm)	$P1$ (dBm)	$P2$ (dBm)	$P1$ (dBm)	$P2$ (dBm)
7.18	7.19	7.53	7.53	8.32	8.33
2.15	2.16	3.52	3.49	3.99	3.99
-2.90	-2.90	-1.45	-1.48	-.98	-.98
-7.85	-7.86	-6.40	-6.49	6.01	5.89
-12.9	-13.3	-11.62	-11.79	-11.24	-11.06

TABLE II
TEST ON 10 dB NOMINAL ON-WAFER
VERIFICATION ATTENUATOR

P_{in} (dBm)	P_{out} (dBm)	$|b_2/a_1|^2$ (dB)
13.83	3.84	-10.01
2.53	-12.52	-10.01
-12.54	-22.55	-10.00
-17.52	-27.52	-10.03
$F = 14$ GHz		
11.75	1.84	-9.90
2.98	-6.92	9.91
-2.97	-12.84	-9.91
-13.03	-22.95	-9.90
$F = 16$ GHz		
11.14	1.42	-9.74
1.47	-8.30	-9.74
-6.43	-16.15	-9.76
-12.43	-22.14	-9.77

The quantity E_G provides another way to compute the input power coefficient $|I_{10}|^2$, which is more practical to implement in the application software and avoids the measurement of $|a_1^M|^2$ to solve (11). Note that from (14), we have

$$|I_{10}|^2 = \frac{|C_{10}|^2}{|E_{10}|^2|E_G|^2} \quad (15)$$

where $|E_{10}|^2$ and $|C_{10}|^2$ are already known from the output port power calibration.

V. EXPERIMENTAL RESULTS

The capability of the test set to measure power levels at the input section was demonstrated on a coaxial system (i.e., without probes) because an on-wafer power sensor was unavailable to make a direct comparison. In order to have a measurement of the input power P_{in}, a power meter was connected at port 1 and its reading was compared with the calibrated network analyzer data. The results for different power levels are reported in Table I. The measurements agree very well for power levels between 10 and 0 dBm, while small discrepancies appear at low powers (less than -10 dBm). This denotes a small imbalance between the responses of the four-channel converter; the test set calibration was carried out with a power level at about 5 dBm.

After an on-wafer calibration where a 1 ps delay through

363

was used, a 10 ± 0.3 dB CPW attenuator verification standard (built by Cascade Microtech) was measured.

The attenuator was loaded at each frequency with $|\Gamma_L|$ ≤ -40 dB provided by appropriately setting a coaxial passive tuner connected at port 5.

The measured values of P_{in}, P_L, and $|(b_2/a_1)|^2$ are reported in Table II. Other on-wafer tests on MMIC TWA and MODFET's were carried out using the same calibration technique, and the results were presented in [7].

VI. Conclusion

The procedure presented in this paper allows one to calibrate, in terms of power and reflection coefficients, a test set designed for measuring on-wafer devices under nonlinear conditions. The coaxial-to-coplanar wafer probe connectors do not need to be disconnected to apply the calibration, and commercial standards both on-wafer and coaxial are used. The procedure is thus particularly useful for automatic test systems at millimetric wavelengths where repetitive disconnections of wafer probes should be avoided. The calibration is also carried out without switching the signal source from the input to the output of the test set.

Appendix A
Output Flow Graphs Derivation

The output directional coupler is modeled as a general four-port reciprocal network. This network, shown in Fig. 5, is terminated at the coupled arms with two fixed loads Γ_3 and Γ_4 (i.e., the input reflection coefficients of the vector network analyzer channels) which have to be taken into account in the output error box model.

If the linearity of the instrument response is assumed [6], the readings r_1 and r_2 are linked to the voltages at the coupled ports 3 and 4 by the following relationships:

$$r_1 = b_3(1 + \Gamma_3)k_1$$
$$r_2 = b_4(1 + \Gamma_4)k_2 \qquad (16)$$

where k_1 and k_2 are general constant complex quantities due to the samplers and down-conversion process.[3]

The four-port loaded network is fully described by

$$b_1 \neq S_{11}a_1 - b_3\Gamma_3 S_{13} - b_4\Gamma_4 S_{14} = \qquad S_{12}a_2$$
$$- S_{12}a_1 - b_3\Gamma_3 S_{23} - b_4\Gamma_4 S_{24} = \qquad S_{22}a_2 - b_2$$
$$- S_{13}a_1 + (1 - \Gamma_3 S_{33})b_3 - b_4\Gamma_4 S_{34} = S_{23}a_2$$
$$- S_{14}a_1 - \Gamma_3 S_{34}b_3 + (1 - \Gamma_4 S_{44})b_4 = S_{24}a_2.$$

$$(17)$$

Defining the following matrices:

$$A = \begin{bmatrix} 1 & -S_{11} & -\Gamma_3 S_{13} & -\Gamma_4 S_{14} \\ 0 & -S_{12} & -\Gamma_3 S_{23} & -\Gamma_4 S_{24} \\ 0 & -S_{13} & (1 - \Gamma_3 S_{33}) & -\Gamma_4 S_{34} \\ 0 & -S_{14} & -\Gamma_3 S_{34} & (1 - \Gamma_4 S_{44}) \end{bmatrix} \qquad (18)$$

[3]Since Γ_3 and Γ_4 are fixed, (16) can also be written as $r_1 = H_1 b_3$ and $r_2 = H_2 b_4$, where H_i are complex constants.
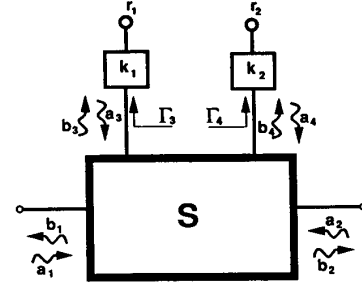

Fig. 5. Output directional coupler network.

$$F = \begin{bmatrix} S_{12} & 0 \\ S_{22} & -1 \\ S_{23} & 0 \\ S_{24} & 0 \end{bmatrix} \qquad (19)$$

$$K = \begin{bmatrix} 0 & 0 & k_1(1 + \Gamma_3) & 0 \\ 0 & 0 & 0 & k_2(1 + \Gamma_4) \end{bmatrix} \qquad (20)$$

$$U = \begin{bmatrix} 1 & 0 & 0 & 0 \\ 0 & 1 & 0 & 0 \end{bmatrix} \qquad (21)$$

and the vectors

$$g = \begin{bmatrix} a_2 \\ b_2 \end{bmatrix} \qquad (22)$$

$$r = \begin{bmatrix} r_1 \\ r_2 \end{bmatrix} \qquad (23)$$

$$p = \begin{bmatrix} b_1 \\ a_1 \\ b_3 \\ b_4 \end{bmatrix} \qquad (24)$$

the linear systems (16) and (17) become

$$r = Kp \qquad (25)$$

$$Ap = Fg. \qquad (26)$$

From (26), it follows that

$$p = A^{-1}Fg. \qquad (27)$$

Equations (27) and (25) give

$$r = KA^{-1}Fg. \qquad (28)$$

Let

$$C = UA^{-1}F \qquad (29)$$

$$D = KA^{-1}F. \qquad (30)$$

From (27) and (28), the two following equations stand:

$$\begin{bmatrix} b_1 \\ a_1 \end{bmatrix} = C \begin{bmatrix} a_2 \\ b_2 \end{bmatrix} \tag{31}$$

$$\begin{bmatrix} r_1 \\ r_2 \end{bmatrix} = D \begin{bmatrix} a_2 \\ b_2 \end{bmatrix}. \tag{32}$$

Note that the C matrix is a transmission matrix of a reciprocal two-port network since it is obtained by the four-port reciprocal one where two ports are loaded by fixed terminations. Thus (31) and (32) can be represented in terms of scattering parameters by the two flow graphs depicted in Fig. 4.

APPENDIX B
CORRECTION FOR NONIDEAL THROUGH LENGTH

The previous evaluations were made under the hypothesis of a through standard, with a para-unitary scattering matrix.

In the general case, a known two-port can be used instead of the ideal through, provided that some calibration formulas are modified.

Let the known two-port scattering matrix be written as

$$\begin{bmatrix} \hat{S}_{11} & \hat{S}_{12} \\ \hat{S}_{21} & \hat{S}_{22} \end{bmatrix}. \tag{33}$$

The input error parameters Ed_1, Es_1, and $Er_1 = I_{10}I_{01}$ are not affected by the nonzero through length since their evaluation is fully carried out by using only on-wafer standard loads connected at the input probe tip.

For a similar reason, the evaluation of the error parameters Ed_2, Es_2, $Er_2 = C_{10}C_{01}$ [Fig. 4(a)] is not affected either since they are also evaluated by measuring coaxial standard loads and the through does not affect the relationship between the traveling voltage waves at port 5 of Fig. 1 and the measured ones b_2^M and a_2^M (i.e., D matrix).

The nonideal through line is only involved when the parameters of the output flow graph of Fig. 4(b) are carried out. Since the input and output probe tips do not correspond, the reflectance measured with the input reflectometer Γ_{in} differs from Γ_L at port 3.

These reflectances are related to each other by the equation

$$\Gamma_{in} = \hat{S}_{11} + \frac{\hat{S}_{12}\hat{S}_{21}\Gamma_L}{1 - \hat{S}_{22}\Gamma_L}. \tag{34}$$

The Γ_L value to be considered for (3) must be first computed by means of (34) from the calibrated value of Γ_{in}. Equation (13) becomes

$$\frac{b_2}{a_1} = \frac{\hat{S}_{21}}{1 - \Gamma_L\hat{S}_{22}} = E_G \frac{(1 - Es_1\Gamma_{in})(1 - E_{11}\Gamma_t)}{1 - Es_2\Gamma_t} \begin{bmatrix} b_2^m \\ a_1^m \end{bmatrix}. \tag{35}$$

Since $b_2 \neq a_1$, E_G is given by

$$E_G = \frac{T(1 - Es_2\Gamma_t)}{(1 - Es_1\Gamma_{in})(1 - E_{11}\Gamma_t)} \frac{1}{\left(\dfrac{b_2^m}{a_1^m}\right)} \tag{36}$$

where

$$T = \frac{\hat{S}_{21}}{1 - \Gamma_L\hat{S}_{22}}. \tag{37}$$

The power correction parameter $|C_{10}|^2$ is not affected by the nonideal through since it again links the measured waves b_2^M to b_t at port 5.

The $|E_{10}|^2$ parameter comes from the Γ_L calibration procedure described above, and finally, the input power correction factor $|I_{10}|^2$ is obtained from (15) using the correct value of E_G, computed with (36).

REFERENCES

[1] R. S. Tucker and P. B. Bradley, "Computer-aided error correction of large-signal load pull measurements," *IEEE Trans. Microwave Theory Techn.*, vol. MTT-32, pp. 296–300, Mar. 1984.

[2] R. Larose, F. Ghannouchi, and R. Bosisio, "A new multi-harmonic load-pull method for non linear device characterization and modeling," in *IEEE MTT-S Dig.*, Dallas, TX, 1990, pp. 443–446.

[3] I. Hecht, "Improved error-correction technique for large-signal load-pull measurement," *IEEE Trans. Microwave Theory Techn.*, vol. MTT-35, pp. 1060–1062, Nov. 1987.

[4] M. E. Goff and C. A. Baratt, "DC to 40 GHz MMIC power sensor," in *12th Annu. GaAs IC Symp. Tech. Dig.*, New Orleans, LA, Oct. 1990, pp. 105–108.

[5] J. Fitzpatrick, "Error models for systems measurement," *Microwave J.*, pp. 63–66, May 1978.

[6] H. J. Eul and B. Schiek, "A generalized theory and new calibration procedures for network analyzer self-calibration," *IEEE Trans. Microwave Theory Tech.*, vol. 39, pp. 724–731, Apr. 1991.

[7] B. Hughes, A. Ferrero, and A. Cognata, "Accurate on-wafer power and harmonic measurements of mm-wave amplifiers and devices," in *IEEE MTT-S Dig.*, Albuquerque, NM, 1992.